One-pot Synthesis of High Value-added Chemicals from Furfural over Bimetal-doped Beta Zeolite and Carbon Solid Acid Catalysts

Yijuan Lu,[a] Wenzhi Li,[a,*] Yuanshuai Zhu,[a] Tingwei Zhang,[a] Qi Zhang,[b] and Qiying Liu [b]

A series of bimetal-doped beta zeolites were prepared *via* a simple post-synthesis strategy including dealumination and metal ion incorporation. The incorporation of ferromagnetic metals into lattice sites of Sn-beta was evidenced by X-ray diffraction (XRD), Fourier transform infrared spectroscopy (FTIR), UV-Vis spectroscopy and X-ray photoelectron spectroscopy (XPS). The high reduction temperature (1094 K) of cobalt in Co-Sn-beta zeolite, as determined by temperature programmed reduction (TPR), confirms that Co interacts strongly with the zeolite support, consistent with lattice tetrahedral (Td) coordination. Co-doped Sn-beta zeolite was found to be a promising Lewis acid catalyst together with a carbon solid acid for the conversion of furfural to isopropyl 4-oxovalerate (i-PL) and γ-valerolactone (GVL). The highest total yield of 92.02% was obtained after reaction for 16 h at 160 °C, including 48.3% i-PL, 37.7% GVL, and 6.0% levulinic acid (LA). The catalysts could also be applied as robust catalysts in glucose conversion to 5-hydromethylfurfural. Zeolite catalysts designed and prepared by this strategy contain multiple metals, enhancing their flexibility and adjustability of function *via* changing the species and ratio of metals to derive optimized catalysts for specific reactions.

Keywords: Transition metals; Sn-beta; Isopropyl 4-oxovalerate; γ-Valerolactone; Furfural

*Contact information: a: Department of Thermal Science and Energy Engineering, University of Science and Technology of China, Hefei 230026, PR China; b: CAS Key Laboratory of Renewable Energy, Guangzhou Institute of Energy Conversion, Chinese Academy of Sciences, Guangzhou 510640, PR China; *Corresponding author: liwenzhi@ustc.edu.cn*

INTRODUCTION

Global climate change and environmental issues have aroused increasing concerns. It is imperative to find good substitutes for fossil resources, such as syngas, biofuel, and bio-oil (Dutta and Pal 2014; Luo *et al*. 2016b; Li *et al*. 2017b). Biomass, one of the most promising renewable energy sources, can be converted into many kinds of biofuels and value-added chemicals (Liu *et al*. 2015; Li *et al*. 2017d). Many studies have been conducted to upgrade bio-oil, which makes it possible to produce liquid hydrocarbons at low cost (Luo *et al*. 2016a; Luo *et al*. 2017). Furfural, derived from pentosan-rich lignocellulosic biomass, is seen as a versatile platform chemical (Cai *et al*. 2014). Furthermore, it can be transformed into many useful chemicals, such as furfuryl alcohol, 2-methylfuran, tetrahydrofuran, cyclopentanone, isopropyl 4-oxovalerate (i-PL), and γ-valerolactone (GVL) (Li *et al*. 2017c; Zhu *et al*. 2017). Notably, GVL has been shown to be an excellent green solvent for biomass-related transformation due to its unique physicochemical properties, such as high boiling point and low melting point, 100% solubility in water, and suppression of char formation (Gürbüz *et al.* 2013; Tang *et*

al. 2014c). It is also hailed as an important building block that can be converted into potential substitutes for fossil fuels and useful chemicals, such as branched alkanes and 1,4-pentanediol (Alonso *et al*. 2013). Isopropyl 4-oxovalerate is supposed to have great potential as a substitute for current additives and solvents derived from petroleum (Démolis *et al*. 2014).

In recent years, GVL and i-PL have been prepared from biomass-derived chemicals, such as levulinic acid (LA), alkyl levulinates, and furfural (Galletti *et al*. 2012; Zhang *et al*. 2012). Different noble metal catalysts (such as Au, Ru, Ir, Pt, Pd) have been applied in the hydrogenation of LA and its esters (Du *et al*. 2011; Li *et al*. 2012; Yan *et al*. 2013; Son *et al*. 2014). Although good yields of GVL have been obtained, these catalysts are rare and expensive, restricting their large-scale application. Moreover, external H_2 or formic acid (FA) is usually required as hydrogen donor (Feng *et al*. 2018; Son *et al*. 2014). The usage of H_2 has been limited by problems related to H_2 storage, and the acidity of FA may cause corrosion of equipment, increasing costs. To overcome these shortcomings, a catalytic transfer hydrogenation (CTH) method for the hydrogenation of LA and alkyl levulinates to GVL over heterogeneous catalysts was reported by Chia and Dumesic (2011), in which secondary alcohols were employed as hydrogen donors. The replacement of H_2 by secondary alcohols and the introduction of non-precious metal catalysts is an economical alternative for GVL production. Compared with LA and ethyl levulinate (EL), furfural has gained increasing attention in such a conversion due to its lower cost and easier preparation. Bui *et al*. (2013) developed a domino reaction for the production of GVL from furfural by using Zr-beta and Al-MFI-ns as a Lewis acid catalyst and Brønsted acid catalyst, respectively. Zhu *et al*. (2016) converted furfural into GVL over Au/ZrO_2 catalyst combined with ZSM-5. Hernández *et al*. (2016) reported the one-pot conversion of furfural into GVL and i-PL with yields of 22.6% and 6.5%, respectively, at 443 K after 24 h using bifunctional Brønsted-Lewis Zr-Al-beta zeolite as catalyst. Winoto *et al*. (2016) found that the mixture of Sn-beta and Al-beta was inefficient when devoted to the furfural transformation with the carbon balance as low as 71.7%.

A Lewis acid is required to achieve the catalytic transfer of hydrogen in one-pot conversion of furfural to GVL (Bui *et al*. 2013). Thus, finding an efficient Lewis acid is of great significance to improving the conversion yield. Some zeolites were supposed to be promising Lewis acid catalysts, as they have been extensively employed in biomass conversion in view of their extraordinary properties, such as large surface area, tunable acidity, and shape-selective microporous structure (Moliner *et al*. 2010; Nikolla *et al*. 2011; Rai *et al*. 2013). Specifically, Sn-beta zeolite has been reported to show high catalytic activity in bio-derived chemical transformation due to its water tolerance and 12-membered ring structure, as well as a mature preparation method (Holm *et al*. 2012; Lew *et al*. 2012; Pagán-Torres *et al*. 2012). However, there was still room for improvement of Sn-beta zeolite over the transformation of furfural into GVL (Bui *et al*. 2013; Winoto *et al*. 2016), so modification of Sn-beta zeolite to promote its performance was necessary. Recently, a simple and convenient routine for the incorporation of various Lewis acid sites into zeolites was developed by Hammond *et al.* (2012). The novel synthesis method demonstrates several advantages over the conventional hydrothermal synthesis route, such as shorter synthesis time and a well-preserved zeolite framework. Additionally, Li *et al*. (2017a) prepared a bimetallic Ni-Fe/AC catalyst to catalyze EL to GVL and achieved a GVL yield of 99.0% under mild reaction conditions. Zhou *et al*. (2015) demonstrated that Co/TiO_2 was efficient in hydrogenation of EL to GVL, and

Varkolu *et al*. (2015) reported that Ni nanoparticles supported on mesoporous silicas with 2D and 3D structures were highly efficient for hydrogenation of LA.

Inspired by this pioneering work (Hammond *et al*. 2012; Varkolu *et al*. 2015; Zhou *et al*. 2015; Li *et al*. 2017a), different amounts of Fe, Co, and Ni were doped into Sn-beta *via* a post-synthetic method in this study. The modified zeolites, combined with Brønsted acid (ion-exchange resin: PTSA-POM), were applied in one-pot conversion of biomass-derived furfural to i-PL and GVL. There is a lack of published information on two metals being doped into the aluminum-free beta framework simultaneously, and the strategy could be applied in other zeolites or metals to derive high-efficiency catalysts. This catalytic system could also be employed for glucose conversion to 5-HMF under mild conditions.

EXPERIMENTAL

Materials

Hβ zeolite (Si/Al = 25) was purchased from Tianjin Nankai Catalyst Co., Ltd. (Tianjin, China). Furfural (99%), paraformaldehyde (POM, AR), p-toluenesulfonic acid monohydrate (PTSA·H_2O, 98.5%), iron (III) acetylacetonate (98%), nickel acetylacetonate (95%), cobalt (III) acetylacetonate (98%), γ-valerolactone (GVL, 98%), ethyl levulinate (99%), levulinic acid (99%), and glucose (≥ 99.5%) were purchased from Aladdin Industrial Inc. (Shanghai, China). Tin (II) acetate was purchased from Sigma-Aldrich Industrial Inc. (Shanghai, China). Isopropanol (AR), H_2SO_4 (96 to 98%, AR), and HNO_3 (65 to 68%, AR) were obtained from Sinopharm Chemical Reagent Co., Ltd. (Shanghai, China). Isopropyl 4-oxovalerate (95%) was purchased from Struchem Co., Ltd. (Jiangsu, China). All reagents were used without further purification.

Catalyst Synthesis and Characterization

First, 2.0 g of Hβ and 40 mL of 13 M HNO_3 were added into a Teflon-lined stainless steel autoclave at 100 °C for 20 h with a rotary speed of 20 rpm. The solid was then filtered and washed with distilled water until the filtrate was neutral and dried under vacuum to obtain the dealuminated beta zeolite (deAlβ).

A series of catalysts, Co-Sn-beta-*x* (*x* = 5, 10, 18, 25; with *x* representing the ratio of Sn to Co), were synthesized *via* the solid-state ion-exchange (SSIE) method. Next, 1.0 g deAlβ was mixed and ground for 20 min with the corresponding amount of cobalt (II) acetylacetonate and tin (II) acetate, and the total amount of these two metal-organic precursors was 0.844 mmol. The mixed powder was then calcined at 550 °C for 4 h under flowing air. The Co-Sn-beta-*x* catalysts were obtained from the corresponding amount of precursors. Further, Ni-Sn-beta-*x* and Fe-Sn-beta-*x* were prepared by the same strategy excepting the substitute of precursor, and the PTSA-POM was synthesized according to Xu *et al*. (2015).

X-ray diffraction (XRD) patterns of zeolite materials were recorded on a SmartLab rotating target diffractometer (Rigaku Corporation, Tokyo, Japan) from 5° to 35°. The functional groups of fresh zeolite catalysts were analyzed by Fourier transform infrared spectroscopy (FTIR) on a Nicolet 8700 (Thermo Nicolet Corporation, Madison, USA), using KBr disks. Transmission electron microscopy (TEM) images were taken on a JEM-2011 microscope (JEOL, Tokyo, Japan) at 200 kV. Temperature-programmed reduction (TPR) and temperature-programmed desorption of ammonia (NH_3- TPD) were

performed on a ChemStar TPx chemisorption analyzer (Thermo Fisher Scientific, Waltham, MA, USA). UV-vis spectra were recorded with a SolidSpec-3700 DUV spectrometer (Shimadzu, Japan). X-ray photoelectron spectroscopy (XPS) was performed using a Thermo-VG Scientific ESCALAB 250 (Waltham, MA, USA).

Experimental Procedure

The catalytic conversion of furfural into i-PL, LA, and GVL was performed in a high-pressure stainless steel reactor (50 mL) equipped with an electric heating mantle under magnetic stirring. In a typical experiment, 0.30 g furfural, 0.20 g *M*-Sn-beta-*x* (M representing Fe, Co, and Ni), 0.2 g PTSA-POM, and 30 mL isopropanol were loaded into the reactor and sealed. The reactor was then heated to the desired temperature in 30 min and kept for different durations with a stirring speed of 600 rpm. Zero time was considered to be the instant when the reaction temperature just reached the given temperature. When the reaction ended, the reactor was immersed in cold water quickly to quench the reaction. Then, phenylethyl alcohol was added as the internal standard and agitated for several minutes. Finally, the samples were collected by filtration using a 0.45 μm syringe prior to gas chromatography (GC) analysis.

To test catalysts' reusability, the mixture was filtrated to obtain the solid catalysts after reaction and then washed with acetone for five consecutive times, followed by drying at 373 K for 12 h before the next run. After five times reuse, the catalyst was washed, dried and calcined at 550 ºC for 4 h under flowing air to remove deposits within its structure, aiming to regenerate its activity. During the calcination, PTSA-POM was oxidized fully due to its resin nature. According to previous work (Xu *et al*. 2015; Li *et al*. 2016), PTSA-POM has an excellent reusability; thus, the introduction of fresh PTSA-POM would not cause obvious influence on the result. Consequently, fresh PTSA-POM was used together with the regenerated zeolite catalyst in run 6.

Glucose transformation was performed in a 25 mL stainless steel reactor under magnetic stirring at a speed of 600 rpm. Typically, 0.4 g glucose, PTSA-POM (0.2 g), and Co-Sn-beta-18 (0.2 g) were loaded into the reactor; then, 1.5 mL distilled water and 15 mL GVL were added into the reactor and sealed. The remaining steps were the same with those of furfural transformation. Finally, the reaction solution was collected by filtration, and the concentrations of HMF, furfural, and glucose were analyzed by high-performance liquid chromatography (HPLC).

Product Analysis

The products were identified on a gas chromatograph / mass spectrometer (GCMS-QP2010S, Shimadzu, Kyoto, Japan) equipped with an Rtx-5MS column (30 m × 25 mm × 0.25 μm). The oven temperature was programmed as 40 °C held for 3 min, increased to 180 °C at 4 °C/min and then to 260 °C at 10 °C/min. Finally, it was held for 10 min. Quantitative analysis of the products was determined by a GC-2010 gas chromatograph (Shimadzu, Kyoto, Japan) with FID detector and WondaCAP5 column. The oven temperature was held at 50 °C for 3 min, increased to 250 °C at 10 °C/min, and then held for 10 min. The product yield was calculated by using phenylethyl alcohol as an internal standard.

Furfural conversion and yields of i-PL, LA, and GVL were defined by Eqs. 1 to 4,

$$\textit{furfural conversion} = (1 - \textit{furfural in products} / \textit{starting furfural}) \times 100\% \quad (1)$$

$$\textit{i-PL yield} = (\textit{i-PL produced} / \textit{starting furfural}) \times 100\% \quad (2)$$

$$LA\ yield = (LA\ produced / starting\ furfural) \times 100\% \quad (3)$$

$$GVL\ yield = (GVL\ produced / starting\ furfural) \times 100\% \quad (4)$$

where *furfural in products*, *starting furfural*, *i-PL produced*, *LA produced*, and *GVL produced* are in moles (mol). Quantitative analysis of glucose, HMF, and furfural was conducted with a Waters HPLC (Waters 515 pump) equipped with an ultraviolet detector (Waters 2489) and refractive index detector (Waters 2414). For HMF and furfural analyses, a Waters Symmetry C18 column was used. The column oven temperature was 30 °C, and the mobile phase was a methanol / distilled water (2/3, v/v) solution with a flow rate of 0.4 mL/min. For glucose analysis, a Waters XBridge™ Amide column was used. Detector and column temperatures were 45 °C, and the mobile phase was an acetonitrile / distilled water (3/2, v/v) solution with a flow rate of 0.4 mL/min. Glucose conversion and yields of HMF were defined by Eqs. 5 and 6, respectively,

$$glucose\ conversion = (1 - glucose\ in\ products / starting\ glucose) \times 100\% \quad (5)$$

$$HMF\ yield = (HMF\ produced / starting\ glucose) \times 100\% \quad (6)$$

where *glucose in products*, *starting glucose*, and *HMF produced* are in moles (mol).

RESULTS AND DISCUSSION

Characterization of the Catalysts

Figure 1 depicts the XRD patterns of parent H-beta, deAl-beta, Sn-beta, Co-Sn-beta-18, Fe-Sn-beta-18, and Ni-Sn-beta-18 zeolites. All samples showed similar diffraction peaks corresponding to BEA topology, demonstrating the preservation of the beta zeolite framework after dealumination and metal incorporation. As shown in Fig. 1, the 2θ value of the ([302] plane) diffraction peak in parent H-beta increased from 22.48° to 22.76° after the dealumination process. It then decreased to different extents with different metals incorporated (Sn-beta (2θ = 22.56°), Co-Sn-beta-18 (2θ = 22.64°), Fe-Sn-beta-18 (2θ = 22.54°), and Ni-Sn-beta-18 (2θ = 22.64°)). The expansion and contraction of the zeolite framework should be attributed to the dealumination and metal incorporation (Dzwigaj *et al*. 2009) and demonstrated the successful incorporation of the metals into the framework of beta zeolite.

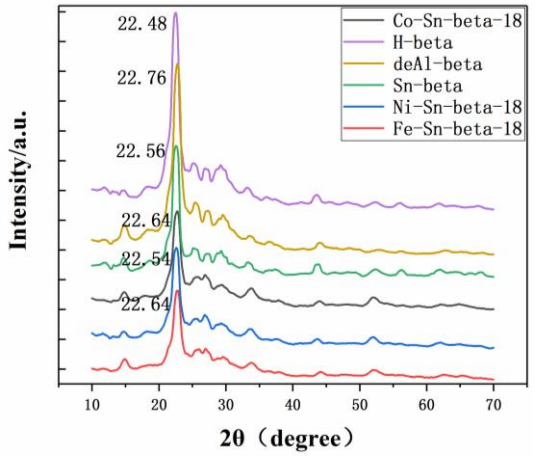

Fig. 1. XRD patterns of selected zeolite samples

Several publications (Tang *et al*. 2014a,b; Song *et al*. 2016) have reported that the incorporation of metals into the dealuminated framework can also be detected by FTIR spectroscopy. Figure 2 shows the FTIR spectra, in which a new peak centered at 950 cm^{-1} appeared in deAl-beta compared to the H-beta due to silanol defects from dealumination (Juttu and Lobo 1999). After the incorporation of different metals, Sn-beta, Co-Sn-beta-18, Fe-Sn-beta-18, and Ni-Sn-beta-18 zeolites were generated and the bond at 950 cm^{-1} disappeared, which is generally considered to be a result the closure of the silanol nests (Hammond *et al*. 2012), in good agreement with XRD analysis results (Fig. 1).

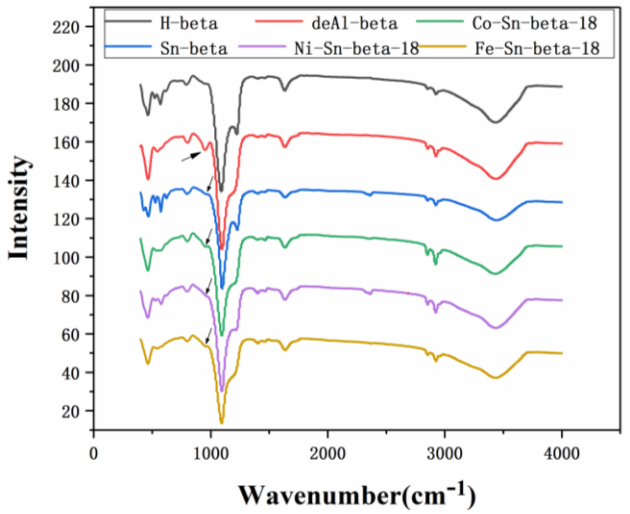

Fig. 2. FTIR transmittance spectra of selected zeolite samples

Table 1. Chemical Composition of Co-Sn-beta-18 Detected by XPS

sample	Co2p (at.%)	Sn3d (at.%)	Si2p (at.%)	C1s (at.%)	O1s (at.%)
Co-Sn-beta-18	0.21	1.03	25.32	13.46	59.98

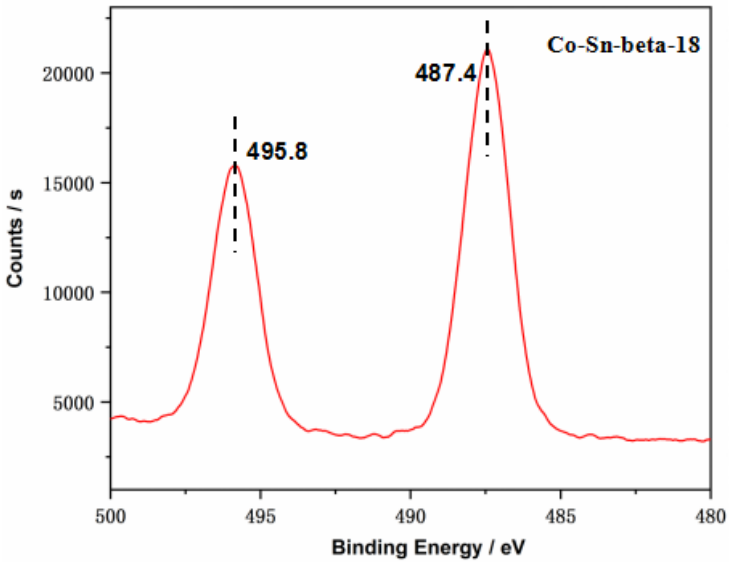

Fig. 3. XPS spectra of Sn 3d of Co-Sn-beta-18 sample

According to the chemical composition of Co-Sn-beta-18 detected by XPS (Table 1), no aluminum species was detected, indicating complete dealumination. What's more, Co and Sn species were detected, verifying their successful incorporation into beta zeolite via the solid-state ion-exchange method, in good agreement with XRD analysis results. The Sn 3d XPS spectrum of Co-Sn-beta-18 sample is measured to provide information on the existing states of Sn species. In Fig. 3, two peaks were observed at 495.8 eV and 487.4 eV, respectively, which should be attributed to $3d_{5/2}$ and $3d_{3/2}$ photoelectrons of tetrahedrally coordinated framework Sn species (Tang *et al*. 2014b).

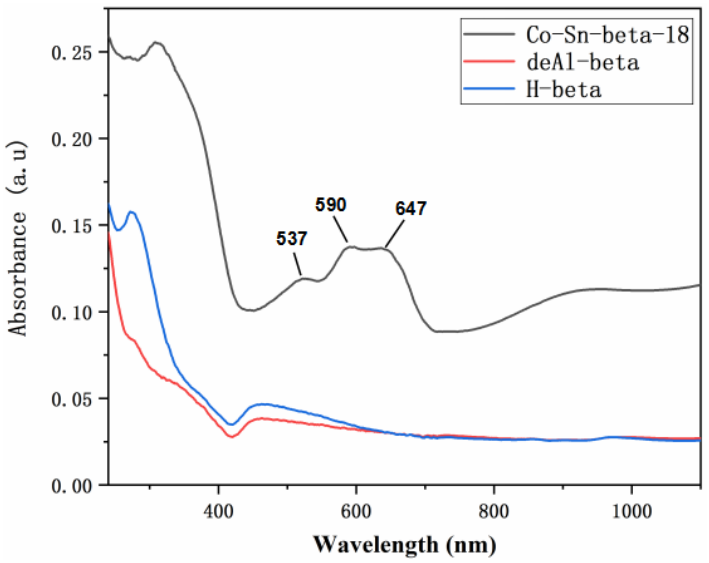

Fig. 4. DR UV-vis spectrum of selected zeolite samples

As shown in Fig. 4, compared with deAl-beta and H-beta, the Co-Sn-beta-18 sample exhibited three UV-vis bands at 537, 590, and 647 nm, which should be attributed to isolated tetrahedral Co (II) species' transition of $^4A_2(^4F) \rightarrow {}^4T_1(^4P)$, $^4A_2(^4F) \rightarrow {}^4T_1(^4F)$, and $^4A_2(^4F) \rightarrow {}^4T_2(^4F)$ respectively (Dzwigaj and Che 2006). Moreover, no signal in the UV-vis spectrum of the band at 516 nm characteristic of Co (II) in octahedral symmetry ($3d^7$ configuration) (El-Malki *et al*. 2000) could be detected. The obtained results suggest the presence of Co species in its II oxidation state and in tetrahedral coordination.

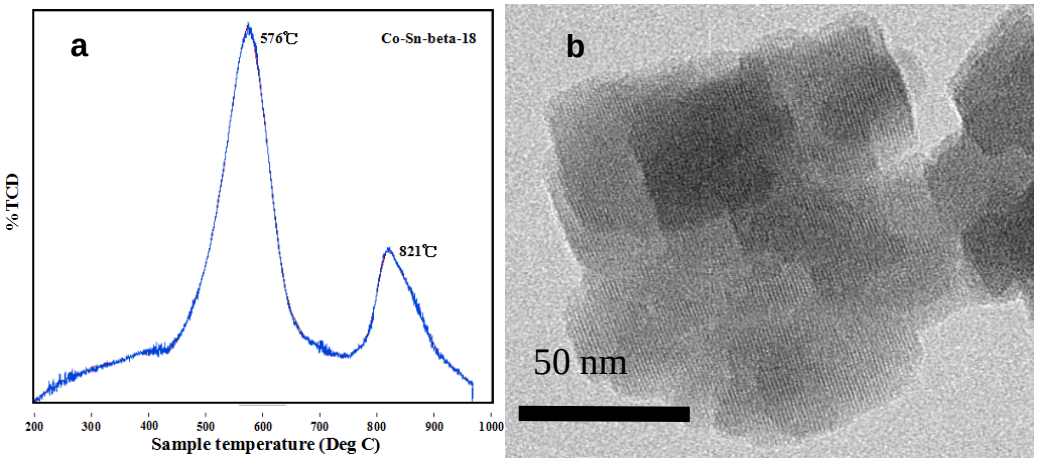

Fig. 5. (a) TPR patterns and (b) TEM image of Co-Sn-beta-18 zeolite

As shown in Fig. 5b, the TEM image of Co-Sn-beta-18 zeolite, the sample appeared as ~100 nm aggregations of nanosheets. High homogeneity of material Co-Sn-beta-18 was observed, without any evidence of SnO_2 or CoO bulk agglomerates, indicating the uniform dispersion of metals. Figure 5a shows the reducibility of Sn and Co species in Co-Sn-beta-18 zeolite pretreated at 623 K in flowing Ar for 0.5 h *via* temperature-programmed reduction (TPR) under flowing hydrogen (10% H_2 in Ar). The TPR pattern of Co-Sn-beta-18 exhibited two peaks at 849 K and 1094 K, attributed to Sn and Co species, respectively. This result indicates that the metals were completely incorporated into the framework in one valence. The very high reduction temperature (1094 K) of cobalt in Co-Sn-beta zeolite determined by TPR confirms that Co interacted strongly with the zeolite support, consistent with lattice tetrahedral (Td) coordination, which is in accordance with the results from UV–vis analysis.

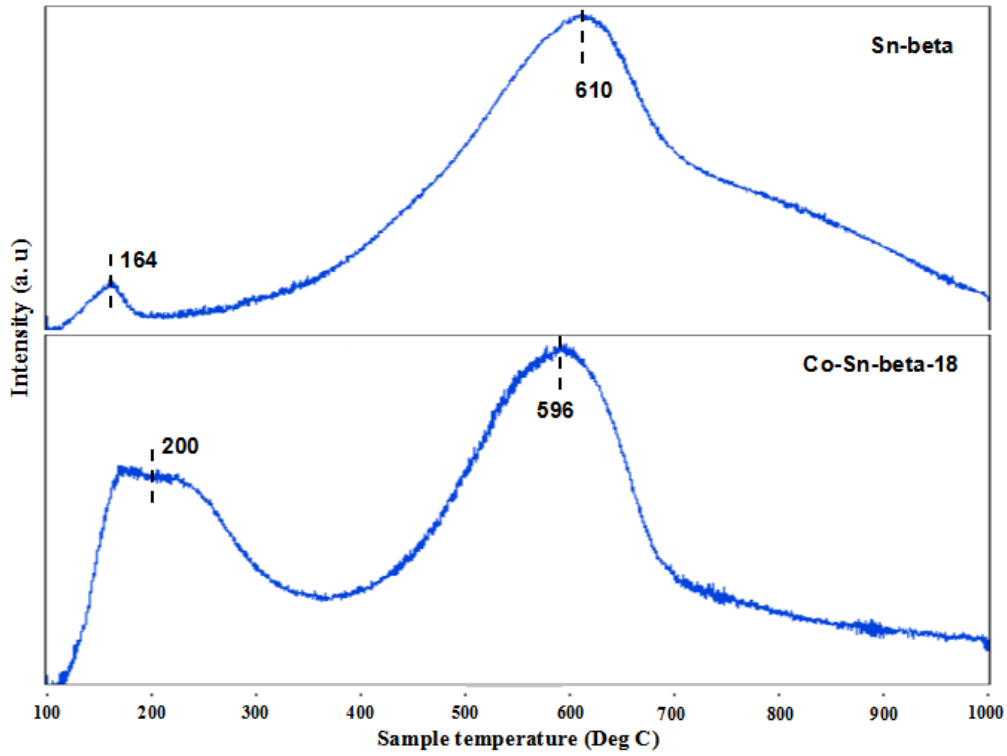

Fig. 6. NH_3-TPD profiles of Sn-beta and Co-Sn-beta-18 samples

The amount and strength of acid sites in Co-Sn-beta-18 and Sn-beta were analyzed by NH_3-TPD, and the results are shown in Fig. 6. Sn-beta zeolite exhibited a wide temperature range of ammonia desorption, and the two desorption peaks centered at 164 and 610 ℃ reveal the presence of weak and strong acid sites respectively. As for Co-Sn-beta-18, two peaks centered at 200 and 596 ℃ can be observed from weak and strong acid sites because of NH_3 desorption. Although these two catalysts have similar total acid sites (Co-Sn-beta-18: 0.45 mmol g^{-1}, Sn-beta : 0.37 mmol g^{-1}), the specific distribution of weak and strong acid sites was widely divergent. After Co species insertion, the density of strong acid sites decreased slightly while the weak acid sites increased markedly and the low temperature peaks were generally ascribed to Lewis acid sites (Lónyi *et al.* 2001). The enhancement of Lewis acid could be beneficial for this reaction.

One-pot Conversion of Furfural into i-PL and GVL over Various Catalysts

To achieve an in-depth understanding of the conversion of furfural to i-PL and GVL catalyzed by different types of Lewis acids along with PTSA-POM, a series of Lewis acids were employed in the reaction, and the results are summarized in Table 2. When the parent H-beta was used as the Lewis acid, the total yield of i-PL and GVL was low due to the low Lewis acidity of H-beta, indicating that stronger Lewis acid sites were required for this reaction. Thus, tin was introduced into the framework first, and the yield of those two products increased sharply with the enhancement of the Lewis acidity of the zeolite catalyst. Zhou *et al*. (2014) reported that Co_3O_4 is very efficient for the hydrogenation of ester levulinate (EL) to GVL under mild conditions. Based on this result, cobalt was doped into the vacancies together with Sn to form Co-Sn-beta (entries 3 to 6). Notably, the proportion of metals has a clear effect on catalytic activity. The yields of i-PL and GVL increased gradually as the ratio of Sn and Co increased from 5 to 18, while the yield began to decrease once the ratio exceeded 18. Furthermore, iron, nickel, and cobalt have similarities in physicochemical properties due to their shared membership in Group VIII, so iron and nickel were also doped, and the corresponding zeolites were used in the reaction (entries 7 to 9). Compared to Co-Sn-beta, the activities of Ni-Sn-beta and Fe-Sn-beta were much lower, especially Fe-Sn-beta, a result consistent with Zhou *et al*. (2014).

Table 2. One-pot Conversion of Furfural into i-PL and GVL over Various Lewis Acids along with PTSA-POM [a]

Entry	Zeolite Catalyst	Furfural Conversion (mol%)	Yield (mol%)			Total Yield (mol%)
			LA	i-PL	GVL	
1	H-beta	100	12.16	30.37	4.78	47.31
2	Sn-beta	100	11.60	58.77	15.17	85.54
3	Co-Sn-beta-5	75.74	5.36	20.12	14.28	39.76
4	Co-Sn-beta-10	100	8.33	41.35	25.31	74.99
5	Co-Sn-beta-18	100	6.02	48.33	37.67	92.02
6	Co-Sn-beta-25	100	8.16	46.25	30.87	85.28
7	Ni-Sn-beta-10	100	7.92	42.78	17.46	68.16
8	Ni-Sn-beta-18	100	10.26	59.28	19.57	89.11
9	Fe-Sn-beta-18	100	6.14	54.14	10.51	70.79

[a]: 3 mmol furfural, 30 mL 2-propanol, 0.2 g PTSA-POM, 0.2 g zeolite catalyst, T = 433 K, 16 h

Based on the literature (Antunes *et al.* 2016; Song *et al.* 2017) and the present experimental results, a possible reaction network (Fig. 7) is depicted.

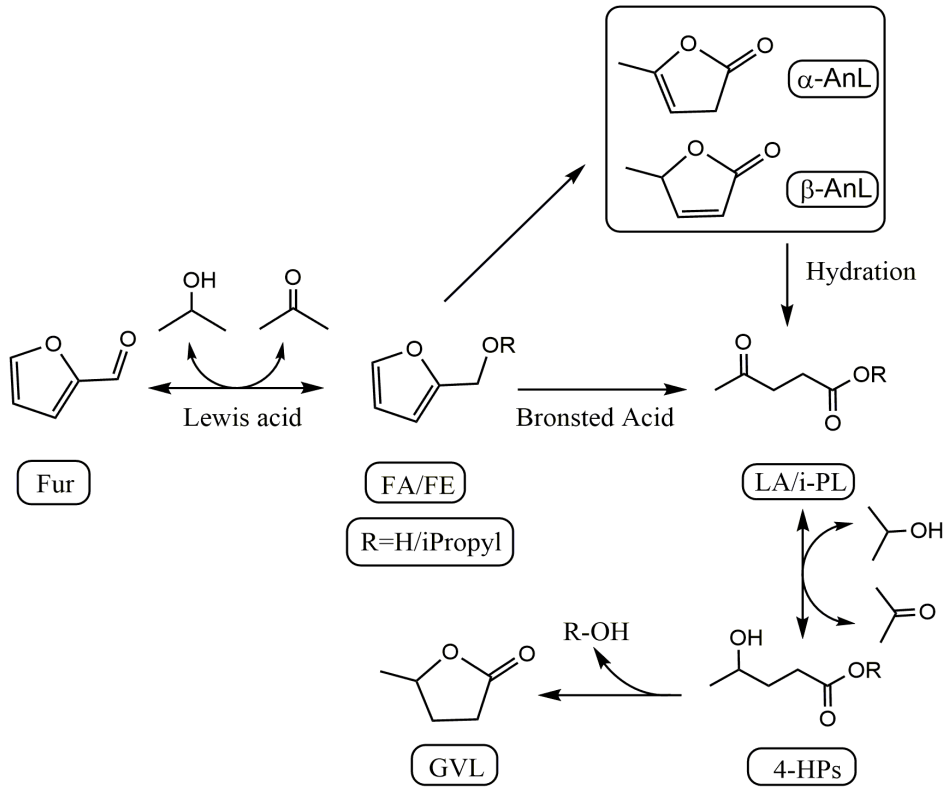

Fig. 7. Reaction network of furfural conversion to GVL

Furfural is used as the initial reactant, while isopropanol is used as the H-donor and solvent. First, furfural is converted into furfuryl alcohol (FA) through a transfer-hydrogenation (TH) process promoted by the Lewis acid catalyst. Due to the presence of the Brønsted acid and isopropanol, partial FA is converted into isopropyl furfuryl ether (FE). Owing to the abundance of i-PL after 8 h, the Brønsted acid turns most of the FA and FE into a mixture of LA and i-PL *via* hydrolytic ring-opening reactions. Next, LA and i-PL undergo a second TH step to produce the corresponding 4-hydroxypentanoates (4-HPs), followed by lactonization to form GVL. Besides, α-angelica lactone (α-AnL) and β-angelica lactone (β-AnL) were also detected, which should be attributed to the rest of the FA and FE turning into α-AnL and β-AnL (Antunes *et al*. 2016). Following this were ring-opening reactions to become LA and i-PL. The remainder of the conversion process was in accordance with the abovementioned steps.

Effects of Metal Species and Reaction Temperature

As temperature is a pivotal factor in chemical reactions, the effects of Sn-beta, Ni-Sn-beta-18, and Co-Sn-beta-18 on product distribution under different temperatures were investigated. As shown in Fig. 8a, when Sn-beta was applied to the system, the temperature required for complete conversion of furfural was 150 °C for Sn-beta, 140 °C for Ni-Sn-beta-18, and 130 °C for Co-Sn-beta-18, indicating that Co- and Ni-doped Sn-beta possessed better catalytic activity.

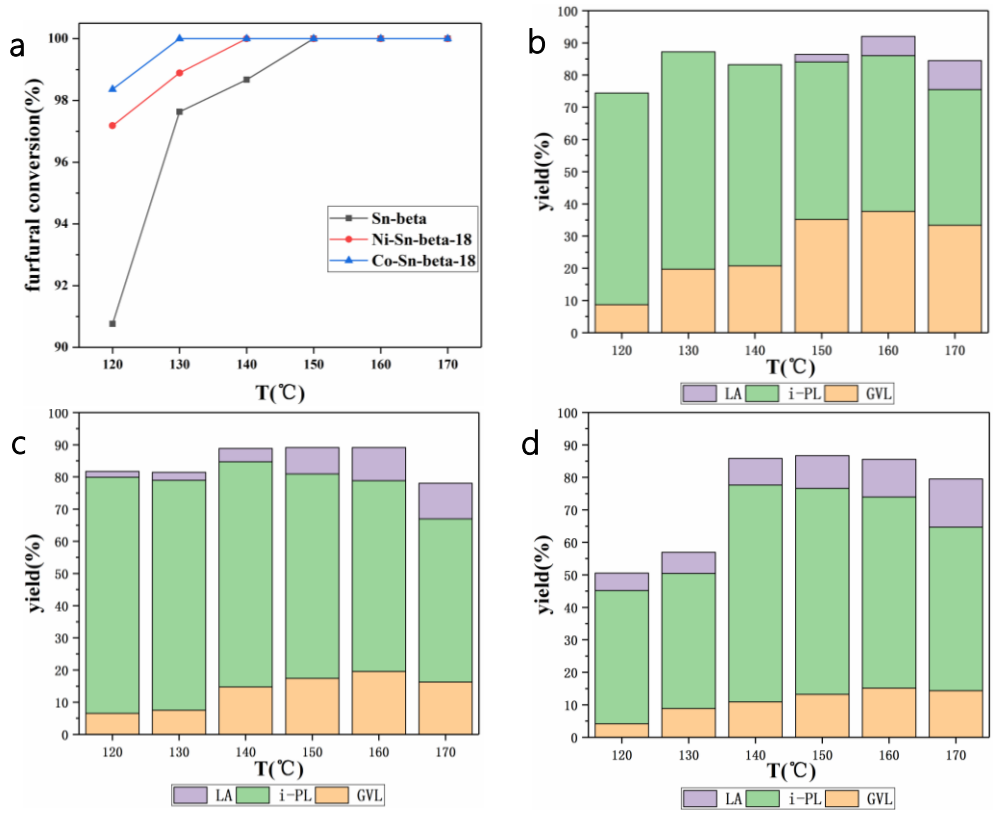

Fig. 8. The effects of reaction temperature on furfural conversion and product yields under different zeolite catalysts: a) temperature vs. furfural conversion, b) Co-Sn-beta-18, c) Ni-Sn-beta-18, d) Sn-beta. Reaction conditions: 3 mmol furfural, 30 mL 2-propanol, 0.2 g PTSA-POM, 0.2 g zeolite catalyst, 16 h

According to Fig. 8b, 8c, and 8d, the yields of i-PL and GVL over Ni-Sn-beta-18 and Co-Sn-beta-18 were greater than those for Sn-beta, especially at relatively low temperatures, demonstrating that the incorporation of Co and Ni could effectively promote the catalytic activity of Sn-beta. A further increase of temperature did not improve the product yield. In contrast, a decrease of total yield was discovered, which may be attributed to more yield-loss reactions. In addition, superior i-PL and GVL yields were obtained using Co-Sn-beta over other two catalysts, as depicted in Fig. 8a, which also verified that the introduction of Co was the best choice among the three metals.

The Effect of Reaction Time

Residence time was also investigated to obtain a better understanding of the conversion process. Based on the relationship between temperature and yields, a series of experiments over Co-Sn-beta-18 catalyst were conducted with the reaction time ranging from 8 h to 24 h (8 h, 12 h, 16 h, 20 h, 24 h), and the results are shown in Fig. 9. In the first 8 h, the yield of i-PL increased dramatically, and little LA was formed, which was related to the strong Brønsted acidity of PTSA-POM. From 8 to 16 h, GVL increased rapidly, and the i-PL yield decreased slowly, probably because i-PL was generated from the substrate constantly and further converted to GVL simultaneously. The peak total yield of 92.1% was obtained at 16 h, and 48.3% i-PL and 37.7% GVL were obtained at 160 °C. After 16 h, the reaction rate slowed down, and a longer reaction time caused a decrease in the total yield.

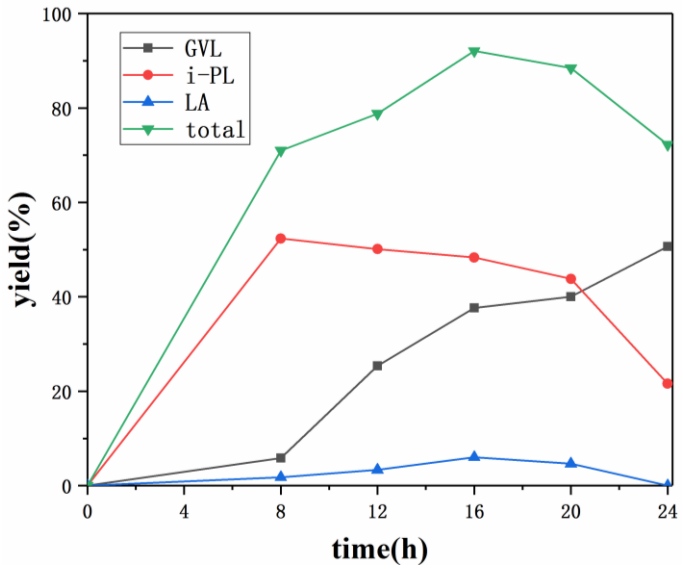

Fig. 9. The effect of reaction time on the product yields. Reaction conditions: 3 mmol furfural, 30 mL 2-propanol, 0.2 g PTSA-POM, 0.2 g Co-Sn-beta-18 catalyst, and 160 °C

Reusability of the Catalyst

The recycling ability of Co-Sn-beta-18 in the conversion of furfural into i-PL and GVL was investigated, with the results shown in Fig. 10. The total yield of entry 1 was 92.1%, while that of entry 5 was 81.9%, and no significant loss could be observed within 5 cycles. The yield of GVL decreased, while LA increased, owing to the catalytic sites' partial deactivation. To verify this conjecture, a calcination regeneration was conducted for the catalyst used 5 times. In run 6, total yield increased to 88.0%, only slightly lower than that of the first use, indicating that the catalytic activity could almost be restored after calcination.

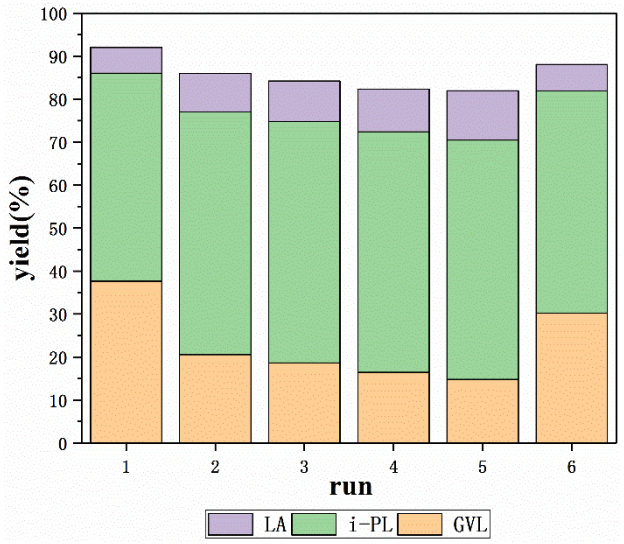

Fig. 10. Recycling test in one-pot catalytic conversion of furfural into i-PL and GVL over Co-Sn-beta-18 zeolite and PTSA-POM. Reaction conditions: 3 mmol furfural, 30 mL 2-propanol, 0.2 g PTSA-POM, 0.2 g Co-Sn-beta-18 catalyst, 16 h, 160 °C

Catalytic Performance on Glucose Transformation

As discussed above, the combination of Co-Sn-beta-18 and PTSA-POM exhibited impressive performance in converting furfural to i-PL and GVL in isopropanol. According to a prior report (Marianou *et al*. 2018), glucose conversion to 5-hydromethylfurfural requires both Lewis acid and Brønsted acid catalysts, so the mixed catalysts were employed in this cascade reaction. As expected, the glucose conversion of 95.6% and a 5-hydromethylfurfural yield of 52.2% were achieved. The Co-Sn-beta-18 zeolite along with PTSA-POM could also be applied as a robust catalyst system in other cascade reactions in biomass transformation, such as glucose into 5-hydromethylfurfural (5-HMF).

CONCLUSIONS

1. A series of bimetal-doped beta zeolites were successfully prepared through a simple post-synthesis strategy including dealumination and metal ion incorporation. Among these zeolites, Fe-doped Sn-beta seemed to have a negative effect on the cascade reaction of furfural conversion, while Co-doped and Ni-doped Sn-beta had a promotion of catalytic activity compared to Sn-beta.
2. Of the tested variants, Co-Sn-beta-18 was selected as a promising Lewis acid catalyst, together with PTSA-POM, for the conversion of furfural to i-PL and γ-valerolactone. The highest total yield of 92.02% (48.33% i-PL, 37.67% GVL, and 6.02% LA) was obtained after reaction for 16 h at 160 °C in isopropanol.

ACKNOWLEDGMENTS

This study was financially supported by the Science and Technological Fund of Anhui Province for Outstanding Youth (1508085J01), the State Key Program of National Natural Science Foundation of China (51536009), and the National Key Technology R&D Program of China (No. 2015BAD15B06).

REFERENCES CITED

Alonso, D. M., Wettstein, S. G., and Dumesic, J. A. (2013). "Gamma-valerolactone, a sustainable platform molecule derived from lignocellulosic biomass," *Green Chem.* 15(3), 584-595. DOI: 10.1039/C3GC37065H

Antunes, M. M., Lima, S., Neves, P., Magalhães, A. L., Fazio, E., Neri, F., and Pillinger, M. (2016). "Integrated reduction and acid-catalysed conversion of furfural in alcohol medium using Zr, Al-containing ordered micro/mesoporous silicates," *Appl. Catal. B: Environ.* 182, 485-503. DOI: 10.1016/j.apcatb.2015.09.053

Bui, L., Luo, H., Gunther, W. R., and Román-Leshkov, Y. (2013). "Domino reaction catalyzed by zeolites with Brønsted and Lewis acid sites for the production of γ-valerolactone from furfural," *Angew. Chem. Int. Edit.* 52(31), 8022-8025. DOI: 10.1002/anie.201302575

Cai, C. M., Zhang, T., Kumar, R., and Wyman, C. E. (2014). "Integrated furfural

production as a renewable fuel and chemical platform from lignocellulosic biomass," *J. Chem. Technol. Biot.* 89(1), 2-10. DOI: 10.1002/jctb.4168

Chia, M., and Dumesic, J. A. (2011). "Liquid-phase catalytic transfer hydrogenation and cyclization of levulinic acid and its esters to γ-valerolactone over metal oxide catalysts," *Chem. Commun.* 47(44), 12233-12235. DOI: 10.1039/C1CC14748J

Démolis, A., Essayem, N., and Rataboul, F. (2014). "Synthesis and applications of alkyl levulinates," *ACS Sustain. Chem. Eng.* 2(6), 1338-1352. DOI: 10.1021/sc500082n

Du, X. L., Bi, Q. Y., Liu, Y.-M., Cao, Y., and Fan, K.-N. (2011). "Conversion of biomass-derived levulinate and formate esters into γ-valerolactone over supported gold catalysts," *ChemSusChem* 4(12), 1838-1843. DOI: 10.1002/cssc.201100483

Dutta, S., and Pal, S. (2014). "Promises in direct conversion of cellulose and lignocellulosic biomass to chemicals and fuels: Combined solvent-nanocatalysis approach for biorefinery," *Biomass Bioenerg.* 62, 182-197. DOI: 10.1016/j.biombioe.2013.12.019

Dzwigaj, S., and Che, M. (2006). "Incorporation of Co (II) in dealuminated BEA zeolite at lattice tetrahedral sites evidenced by XRD, FTIR, diffuse reflectance UV−Vis, EPR, and TPR," *J. Phys. Chem. B* 110(25), 12490-12493. DOI: 10.1021/jp0623387

Dzwigaj, S., Janas, J., Gurgul, J., Socha, R. P., Shishido, T., and Che, M. (2009). "Do Cu (II) ions need Al atoms in their environment to make CuSiBEA active in the SCR of NO by ethanol or propane? A spectroscopy and catalysis study," *Appl. Catal. B: Environ.* 85(3), 131-138. DOI: 10.1016/j.apcatb.2008.07.003

El-Malki, E. M., Werst, D., Doan, P. E., and Sachtler, W. M. (2000). "Coordination of Co^{2+} cations inside cavities of zeolite MFI with lattice oxygen and adsorbed ligands," *J. Phys Chem. B* 104(25), 5924-5931. DOI: 10.1021/jp000540i

Feng, J., Gu, X., Xue, Y., Han, Y., and Lu, X. (2018). "Production of γ-valerolactone from levulinic acid over a Ru/C catalyst using formic acid as the sole hydrogen source," *Sci. Total Environ.* 633, 426-432. DOI: 10.1016/j.scitotenv.2018.03.209

Galletti, A. M. R., Antonetti, C., De Luise, V., and Martinelli, M. (2012). "A sustainable process for the production of γ-valerolactone by hydrogenation of biomass-derived levulinic acid," *Green Chem.* 14(3), 688-694. DOI: 10.1039/C2GC15872H

Gürbüz, E. I., Gallo, J. M. R., Alonso, D. M., Wettstein, S. G., Lim, W. Y., and Dumesic, J. A. (2013). "Conversion of hemicellulose into furfural using solid acid catalysts in γ-valerolactone," *Angew. Chem. Int. Edit.* 52(4), 1270-1274. DOI: 10.1002/anie.201207334

Hammond, C., Conrad, S., and Hermans, I. (2012). "Simple and scalable preparation of highly active lewis acidic Sn-β," *Angew. Chem. Int. Edit.* 51(47), 11736-11739. DOI: 10.1002/anie.201206193

Hernández, B., Iglesias, J., Morales, G., Paniagua, M., López-Aguado, C., Fierro, J. L. G., Wolf, P., Hermans, I., and Melero, J. A. (2016). "One-pot cascade transformation of xylose into γ-valerolactone (GVL) over bifunctional Brønsted-Lewis Zr-Al-beta zeolite," *Green Chem.* 18(21), 5777-5781. DOI: 10.1039/C6GC01888B

Holm, M. S., Pagán-Torres, Y. J., Saravanamurugan, S., Riisager, A., Dumesic, J. A., and Taarning, E. (2012). "Sn-beta catalysed conversion of hemicellulosic sugars," *Green Chem.* 14(3), 702-706. DOI: 10.1039/C2GC16202D

Juttu, G. G., and Lobo, R. F. (1999). "Framework modification of microporous silicates *via* gas-phase treatment with $ZrCl_4$," *Catal. Lett.* 62(2-4), 99-106. DOI: 10.1023/A:1019047022166

Lew, C. M., Rajabbeigi, N., and Tsapatsis, M. (2012). "One-pot synthesis of 5-

(ethoxymethyl)furfural from glucose using Sn-BEA and Amberlyst catalysts," *Ind. Eng. Chem. Res.* 51(14), 5364-5366. DOI: 10.1021/ie2025536

Li, C., Xu, G., Zhai, Y., Liu, X., Ma, Y., and Zhang, Y. (2017a). "Hydrogenation of biomass-derived ethyl levulinate into γ-valerolactone by activated carbon supported bimetallic Ni and Fe catalysts," *Fuel* 203, 23-31. DOI: 10.1016/j.fuel.2017.04.082

Li, M., Li, W., Lu, Y., Jameel, H., Chang, H.-M., and Ma, L. (2017b). "High conversion of glucose to 5-hydroxymethylfurfural using hydrochloric acid as a catalyst and sodium chloride as a promoter in a water/γ-valerolactone system," *RSC Adv.* 7(24), 14330-14336. DOI: 10.1039/C7RA00701A

Li, W., Xie, J.-H., Lin, H., and Zhou, Q.-L. (2012). "Highly efficient hydrogenation of biomass-derived levulinic acid to γ-valerolactone catalyzed by iridium pincer complexes," *Green Chem.* 14(9), 2388-2390. DOI: 10.1039/C2GC35650C

Li, W., Xu, Z., Zhang, T., Li, G., Jameel, H., Chang, H.-M., and Ma, L. (2016). "Catalytic conversion of biomass-derived carbohydrates into 5-hydroxymethyl-furfural using a strong solid acid catalyst in aqueous γ-valerolactone," *BioResources* 11(3), 5839-5853. DOI: 10.15376/biores.11.3.5839-5853

Li, W., Zhu, Y., Lu, Y., Liu, Q., Guan, S., Chang, H.-M., Jameel, H., and Ma, L. (2017c). "Enhanced furfural production from raw corn stover employing a novel heterogeneous acid catalyst," *Bioresource Technol.* 245, 258-265. DOI: 10.1016/j.biortech.2017.08.077

Li, Y., Su, D., Luo, S., Luo, Y., and Xu, Q. (2017d). "Pyrolysis gas as a carbon source for biogas production via anaerobic digestion," *RSC Adv.* 7(66), 41889-41895. DOI:10.1039/c7ra08559a

Liu, Y., Chen, L., Wang, T., Zhang, Q., Wang, C., Yan, J., and Ma, L. (2015). "One-pot catalytic conversion of raw lignocellulosic biomass into gasoline alkanes and chemicals over $LiTaMoO_6$ and Ru/C in aqueous phosphoric acid," *ACS Sustain. Chem. Eng.* 3(8), 1745-1755. DOI: 10.1021/acssuschemeng.5b00256

Lónyi, F., and Valyon, J. (2001). "A TPD and IR study of the surface species formed from ammonia on zeolite H-ZSM-5, H-mordenite and H-beta," *Thermochim. acta,* 373(1), 53-57. DOI: 10.1016/S0040-6031(01)00458-0

Luo, Y., Guda, V. K., Hassan, E. B., Steele, P. H., Mitchell, B., and Yu, F. (2016a). "Hydrodeoxygenation of oxidized distilled bio-oil for the production of gasoline fuel type," *Energy Convers. Manage.* 112, 319-327. DOI: 10.1016/j.enconman.2015.12.047

Luo, Y., Hassan, E. B., Guda, V., Wijayapala, R., and Steele, P. H. (2016b). "Upgrading of syngas hydrotreated fractionated oxidized bio-oil to transportation grade hydrocarbons," *Energy Convers. Manage.* 115, 159-166. DOI: 10.1016/j.enconman.2016.02.051

Luo, Y., Hassan, E. B., Miao, P., Xu, Q., and Steele, P. H. (2017). "Effects of single-stage syngas hydrotreating on the physical and chemical properties of oxidized fractionated bio-oil," *Fuel* 209: 634-642. DOI: 10.1016/j.fuel.2017.07.114

Marianou, A. A., Michailof, C. M., Pineda, A., Iliopoulou, E. F., Triantafyllidis, K. S., and Lappas, A. A. (2018). "Effect of Lewis and Brønsted acidity on glucose conversion to 5-HMF and lactic acid in aqueous and organic media," *Appl. Catal. A-General* 555, 75-87. DOI: 10.1016/j.apcata.2018.01.029

Moliner, M., Román-Leshkov, Y., and Davis, M. E. (2010). "Tin-containing zeolites are highly active catalysts for the isomerization of glucose in water," *P. Natl. Acad. Sci. USA* 107(14), 6164-6168. DOI: 10.1073/pnas.1002358107

Nikolla, E., Román-Leshkov, Y., Moliner, M., and Davis, M. E. (2011). "'One-pot' synthesis of 5-(hydroxymethyl)furfural from carbohydrates using tin-beta zeolite," *ACS Catal.* 1(4), 408-410. DOI: 10.1021/cs2000544

Pagán-Torres, Y. J., Wang, T., Gallo, J. M. R., Shanks, B. H., and Dumesic, J. A. (2012). "Production of 5-hydroxymethylfurfural from glucose using a combination of Lewis and Brønsted acid catalysts in water in a biphasic reactor with an alkylphenol solvent," *ACS Catal.* 2(6), 930-934. DOI: 10.1021/cs300192z

Rai, N., Caratzoulas, S., and Vlachos, D. G. (2013). "Role of silanol group in Sn-beta zeolite for glucose isomerization and epimerization reactions," *ACS Catal.* 3(10), 2294-2298. DOI: 10.1021/cs400476n

Son, P. A., Nishimura, S., and Ebitani, K. (2014). "Production of γ-valerolactone from biomass-derived compounds using formic acid as a hydrogen source over supported metal catalysts in water solvent," *RSC Adv.* 4(21), 10525-10530. DOI: 10.1039/C3RA47580H

Song, S., Di, L., Wu, G., Dai, W., Guan, N., and Li, L. (2017). "Meso-Zr-Al-beta zeolite as a robust catalyst for cascade reactions in biomass valorization," *Appl. Catal. B: Environ.* 205, 393-403. DOI: 10.1016/j.apcatb.2016.12.056

Song, S., Wu, G., Dai, W., Guan, N., and Li, L. (2016). "Al-free Fe-beta as a robust catalyst for selective reduction of nitric oxide by ammonia," *Catal. Sci. Technol.* 6(23), 8325-8335. DOI: 10.1039/C6CY02124G

Tang, B., Dai, W., Sun, X., Guan, N., Li, L., and Hunger, M. (2014a). "A procedure for the preparation of Ti-Beta zeolites for catalytic epoxidation with hydrogen peroxide," *Green Chem.* 16(4), 2281-2291. DOI: 10.1039/C3GC42534G

Tang, B., Dai, W., Wu, G., Guan, N., Li, L., and Hunger, M. (2014b). "Improved postsynthesis strategy to Sn-Beta zeolites as Lewis acid catalysts for the ring-opening hydration of epoxides," *ACS Catal.* 4(8), 2801-2810. DOI: 10.1021/cs500891s

Tang, X., Zeng, X., Li, Z., Hu, L., Sun, Y., Liu, S., Lei, T., and Lin, L. (2014c). "Production of γ-valerolactone from lignocellulosic biomass for sustainable fuels and chemicals supply," *Renew. Sust. Energ. Rev.* 40, 608-620. DOI: 10.1016/j.rser.2014.07.209

Varkolu, M., Velpula, V., Ganji, S., Burri, D. R., and Kamaraju, S. R. R. (2015). "Ni nanoparticles supported on mesoporous silica (2D, 3D) architectures: Highly efficient catalysts for the hydrocyclization of biomass-derived levulinic acid," *RSC Adv.* 5(70), 57201-57210. DOI: 10.1039/C5RA10857H

Winoto, H. P., Ahn, B. S., and Jae, J. (2016). "Production of γ-valerolactone from furfural by a single-step process using Sn-Al-Beta zeolites: Optimizing the catalyst acid properties and process conditions," *J. Ind. Eng. Chem.* 40, 62-71. DOI: 10.1016/j.jiec.2016.06.007

Xu, Z., Li, W., Du, Z., Wu, H., Jameel, H., Chang, H.-M., and Ma, L. (2015). "Conversion of corn stalk into furfural using a novel heterogeneous strong acid catalyst in γ-valerolactone," *Bioresource Technol.* 198, 764-771. DOI: 10.1016/j.biortech.2015.09.104

Yan, K., Lafleur, T., Wu, G., Liao, J., Ceng, C., and Xie, X. (2013). "Highly selective production of value-added γ-valerolactone from biomass-derived levulinic acid using the robust Pd nanoparticles," *Appl. Catal. A-Gen.* 468, 52-58. DOI: 10.1016/j.apcata.2013.08.037

Zhang, J., Wu, S., Li, B., and Zhang, H. (2012). "Advances in the catalytic production of valuable levulinic acid derivatives," *ChemCatChem* 4(9), 1230-1237. DOI:

10.1002/cctc.201200113

Zhou, H., Song, J., Fan, H., Zhang, B., Yang, Y., Hu, J., Zhu, Q., and Han, B. (2014). "Cobalt catalysts: Very efficient for hydrogenation of biomass-derived ethyl levulinate to gamma-valerolactone under mild conditions," *Green Chem.* 16(8), 3870-3875. DOI: 10.1039/C4GC00482E

Zhou, H., Song, J., Kang, X., Hu, J., Yang, Y., Fan, H., Meng, Q., and Han, B. (2015). "One-pot conversion of carbohydrates into gamma-valerolactone catalyzed by highly cross-linked ionic liquid polymer and Co/TiO_2," *RSC Adv.* 5(20), 15267-15273. DOI: 10.1039/C4RA14363A

Zhu, S., Xue, Y., Guo, J., Cen, Y., Wang, J., and Fan, W. (2016). "Integrated conversion of hemicellulose and furfural into γ-valerolactone over Au/ZrO_2 catalyst combined with ZSM-5," *ACS Catal.* 6(3), 2035-2042. DOI: 10.1021/acscatal.5b02882

Zhu, Y., Li, W., Lu, Y., Zhang, T., Jameel, H., Chang, H.-M., and Ma, L. (2017). "Production of furfural from xylose and corn stover catalyzed by a novel porous carbon solid acid in γ-valerolactone," *RSC Adv.* 7(48), 29916-29924. DOI: 10.1039/C7RA03995F

Article submitted: March 25, 2018; Peer review completed: May 29, 2018; Revised version received and accepted: June 7, 2018; Published: June 13, 2018.
DOI: 10.15376/biores.13.3.5925-5941